

Yagi-Uda Combined Radiating Structures of Centimeter and Millimeter Wave Band

Sergey L. Berdnik, Victor A. Katrich, Mikhail V. Nesterenko*,
Yuriy M. Penkin, and Oleksandr M. Dumin

Abstract—An electrodynamically rigorous mathematical model of a combined vibrator-slot structure consisting of a narrow radiating slot cut in a rectangular waveguide end wall and several thin impedance vibrators placed over the infinite screen is presented. Numerical results concerning internal and external electrodynamic characteristics of the antennas with optimized structural parameters have confirmed the possibility of constructing the Yagi-Uda combined radiating structures in the microwave and extremely high frequency (EHF) bands.

1. INTRODUCTION

Radiating arrays known as Yagi-Uda (wave-channel) antennas have been widely used in practice throughout the last century. The successful use of Yagi-Uda structures has started with invention of linear vibrator arrays [1]. In the classic version, the antenna consists of an active element, a passive reflector, and several vibrator directors. The number of vibrator directors can be quite large, since each of them guides scattered fields to the next vibrator director, providing the necessary conditions for their excitation. The best array directivity can be achieved by selecting its geometrical parameters: the length of vibrator directors and the distances between them along the longitudinal array axis [2]. The electrodynamic model of the Yagi-Uda antennas with perfectly conducting elements was developed in [3] based on the analytical solution of integral equations for currents on thin vibrators. Later, the authors of this article generalized the model for analyzing the characteristics of the Yagi-Uda antennas with impedance vibrators [4].

The structural diversity of Yagi-Uda antennas is not limited by using only electric elements. The principle of the wave channel antenna was applied to magnetic type elements. For example, an antenna consisting of loop elements, i.e., electrodynamic equivalents of magnetic dipoles, was considered in [5]. This loop antenna consists of a reflector, an active element, and vibrator directors coaxially placed in parallel on the common rod so that they are dielectrically isolated from one another. All loop elements are open-ended with a minimal clearance, and their planes are parallel. A more complex design of the loop wave channel was proposed in [6], where the symmetric antenna elements relative to the longitudinal antenna axis are made in the form of grouped pairs of loop radiators. The Yagi-Uda antennas with a vibrator or loop elements are usually used in the meter and decimeter wavelength ranges. First of all, this is related to the physical principles of radiation by the active elements and the power supply implemented by using coaxial cables. It should also be noted that to minimize the design dimensions of the Yagi-Uda antennas in the decimeter wavelength range, microstrip device based on low-profile structures have been proposed [7, 8].

Received 15 April 2020, Accepted 14 May 2020, Scheduled 7 June 2020

* Corresponding author: Mikhail V. Nesterenko (Mikhail.V.Nesterenko@gmail.com).

The authors are with the Department of Radiophysics, Biomedical Electronics and Computer Systems, V. N. Karazin Kharkiv National University, 4, Svobody Sq., Kharkiv 61022, Ukraine.

The wave channel radiating structures can be used in the microwave and EHF bands under two conditions: the power should be supplied to the antenna by the waveguides, and the magnetic elements must be applied. These conditions were realized in antenna design developed in [9, 10]: apertures of rectangular waveguides were proposed to use as antenna structure elements [9], and slots in microstrip metal patches were excited by a plane dielectric waveguide [10]. However, this type of antennas operating in the centimeter wave band is characterized by insufficient isolation of cross-polarization components, required for remote sensing and wave polarimetry. To minimize this drawback, electrically thin radiating elements should be used in these antennas.

The microwave antennas with linear elements with good polarization isolation can be built based on combined vibrator-slot radiating structures [11]. Electrodynamic characteristics of these radiating structures with waveguide excitation can be easily obtained by a generalized method of induced electromagnetic motive forces (EMMF) [12]. Unfortunately, such an approach for this problem solution was never discussed earlier. The article is aimed at developing, based on the mathematical model, a Yagi-Uda combined vibrator-slot radiating structure (YUCVSRS) operating in the centimeter and millimeter wave ranges. The antenna characteristics will be modelled by a generalized method of induced EMMF, since modelling conducted by existing commercial programs is resource-intensive and low-efficient.

2. FORMULATION AND SOLUTION OF THE DIFFRACTION PROBLEM

Let the H_{10} -wave propagates in a semi-infinite rectangular waveguide (marked by index Wg) from the direction $z = -\infty$. A narrow longitudinal slot cut in the waveguide end wall symmetrically with respect to the side walls and oriented along the axis $\{0x\}$ radiates into the half-space above the infinite perfectly conducting plane (marked by index Hp). In a system of N thin impedance vibrators each of them is placed at fixed distances z_n from the plane as shown in Fig. 1. The cross section of the waveguide is $\{a \times b\}$; the material parameters of the medium filling the waveguide are ε_1, μ_1 ; the slot length and width are $2L_0$ and d . The length and radius of the vibrator with the number $n \in [1, N]$ are $2L_n$ and r_n . The monochromatic fields and currents depend on time t as $e^{i\omega t}$ (ω is the circular frequency).

Let us assume that dimensions of the slot and vibrators satisfy the following inequalities $\frac{r_n}{2L_n} \ll 1$, $\frac{d}{2L_0} \ll 1$, $\frac{d}{\lambda_{1(2)}} \ll 1$ (the $\lambda_{1(2)}$ are wavelengths in the media with parameters $\varepsilon_{1(2)}, \mu_{1(2)}$). Since the electric currents $J_n(s_n)$ on the vibrators and the equivalent magnetic current in the slot $J_0(s_0)$ should

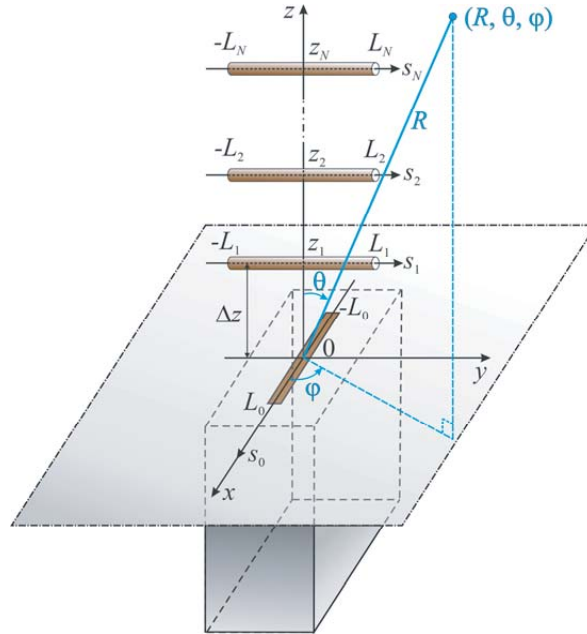


Figure 1. The YUCVSRS geometry and accepted notations.

satisfy the boundary conditions $J_n(\pm L_n) = 0$, $J_0(\pm L_0) = 0$, the initial system of integral equations relative to unknown currents [4, 13] can be written as

$$\begin{aligned} & \left(\frac{d^2}{ds_n^2} + k_2^2 \right) \left\{ \int_{-L_1}^{L_1} J_1(s'_1) G_{s'_1}^{HsE}(s_n, s'_1) ds'_1 + \int_{-L_2}^{L_2} J_2(s'_2) G_{s'_2}^{HsE}(s_n, s'_2) ds'_2 + \dots \right. \\ & \left. + \int_{-L_N}^{L_N} J_N(s'_N) G_{s'_N}^{HsE}(s_n, s'_N) ds'_N \right\} - ik \vec{e}_{s_n} \text{rot} \int_{-L_0}^{L_0} J_0(s'_0) G_{s'_0}^{HsM}(s_n, s'_0) ds'_0 \\ = & i\omega \varepsilon_2 z_{in}(s_n) J_n(s_n), \quad n = 1, 2, \dots, N; \\ & \frac{1}{\mu_1} \left(\frac{d^2}{ds_0^2} + k_1^2 \right) \int_{-L_0}^{L_0} J_0(s'_0) G_{s'_0}^{WgM}(s_0, s'_0) ds'_0 + \frac{1}{\mu_2} \left(\frac{d^2}{ds_0^2} + k_2^2 \right) \int_{-L_0}^{L_0} J_0(s'_0) G_{s'_0}^{HsM}(s_0, s'_0) ds'_0 \\ & + ik \vec{e}_{s_0} \text{rot} \sum_{n=1}^N \int_{-L_n}^{L_n} J_n(s'_n) G_{s'_n}^{HsE}(s_0, s'_n) ds'_n = -i\omega H_{0s_0}(s_0), \end{aligned} \quad (1)$$

where $z_{in}(s_n)$ are the vibrator internal linear impedances, measured in [Ohm/m]; $H_{0s_0}(s_0)$ is the projection of the external source field on the slot axis; $G_{s'_m}^{HsE}(s_n, s'_m)$ and $G_{s'_m}^{HsM, WgM}(s_n, s'_m)$ are components of the electric and magnetic tensor Green's functions (marked by indices E , [12] and M , [14]) for the vector potentials of coupling electrodynamic volumes (half-space above an infinite ideally conducting plane and a semi-infinite rectangular waveguide); $k = 2\pi/\lambda$, λ is the wavelength in free space; \vec{e}_{s_0} , \vec{e}_{s_n} are unit vectors directed along the slot and vibrator axes; and s_0 , s_n are local coordinates associated with the longitudinal axes of the slot and vibrators. The magnetic Green's function in Hs

can be presented as $G_{s'_0}^{HsM}(s_0, s'_0) = \frac{2e^{-ik\sqrt{(s_0-s'_0)^2+(d_e/4)^2}}}{\sqrt{(s_0-s'_0)^2+(d_e/4)^2}}$ where $d_e = de^{-\frac{\pi h}{2d}}$ is the effective slot width

allowing to take into account the actual thickness of the waveguide wall h [14].

Since the projection of the field of external sources on the slot axis is $H_{0s_0}(s_0) = H_0 \cos \frac{\pi s_0}{a} = H_0^s(s_0)$, the magnetic current in the slot can be described by a symmetric function $J_0(s_0) = J_0^s(s_0)$ relative to the slot center. Then, Equation (1) under condition $\varepsilon_{1(2)} = \mu_{1(2)} = 1$ can be transformed to

$$\begin{aligned} & \left(\frac{d^2}{ds_n^2} + k^2 \right) \left\{ \int_{-L_1}^{L_1} J_1(s'_1) G_{s'_1}^{HsE}(s_n, s'_1) ds'_1 + \int_{-L_2}^{L_2} J_2(s'_2) G_{s'_2}^{HsE}(s_n, s'_2) ds'_2 + \dots \right. \\ & \left. + \int_{-L_N}^{L_N} J_N(s'_N) G_{s'_N}^{HsE}(s_n, s'_N) ds'_N \right\} + ik \int_{-L_0}^{L_0} J_0^s(s'_0) \tilde{G}_{s'_0}^{HsM}(s_n, s'_0) ds'_0 \\ = & i\omega z_{in}(s_n) J_n(s_n), \quad n = 1, 2, \dots, N; \\ & \left(\frac{d^2}{ds_0^2} + k_1^2 \right) \int_{-L_0}^{L_0} J_0^s(s'_0) [G_{s'_0}^{WgM}(s_0, s'_0) + G_{s'_0}^{HsM}(s_0, s'_0)] ds'_0 \\ & - ik \sum_{n=1}^N \int_{-L_n}^{L_n} J_n(s'_n) \tilde{G}_{s'_n}^{HsE}(s_0, s'_n) ds'_n = -i\omega H_0^s(s_0). \end{aligned} \quad (2)$$

where $\tilde{G}_{s'_n}^{HsE}(s_0, s'_n) = -\frac{\partial}{\partial z} G_{s'_n}^{HsE}(s_0, 0, z; 0, s'_n, z_n) \Big|_{z=0}$, $\tilde{G}_{s'_0}^{HsM}(s_n, s'_0) = \frac{\partial}{\partial z} G_{s'_0}^{HsM}(0, s_n, z; s'_0, 0, 0) \Big|_{z=z_n}$. In the above expressions, the fixed values of the variable z are substituted after differentiation.

The equations system (2) can be solved by the generalized method of induced EMMF [11, 13], using the functions $J_n(s_n) = J_{0n} f_n(s_n)$ and $J_0^s(s_0) = J_{00}^s f_0^s(s_0)$ as approximating expressions for the

currents. In this expression, J_{0n} and J_{00}^s are unknown complex current amplitudes, and $f_n(s_n)$ and $f_0^s(s_0)$ are predefined basic functions of current distributions, which can be obtained as the solution of the equation defining the currents on the standalone vibrator and slot by the averaging method [12, 14]. The expressions for the YUCVRS can be written as

$$f_n(s_n) = \cos \tilde{k}_n s_n - \cos \tilde{k}_n L_n, \quad f_0^s(s_0) = \cos k s_0 - \cos k L_0, \quad (3)$$

where $\tilde{k}_n = k + \frac{i\alpha_n 2z_{in}^{av}}{60 \text{ Ohm}}$, $\alpha_n = \frac{1}{2 \ln[r_n/(2L_n)]}$ are natural small parameters, and $z_{in}^{av} = \frac{1}{2L_n} \int_{-L_n}^{L_n} z_{in}(s_n) ds_n$ are internal impedances averaged over the vibrators.

Let us apply the generalized method of the induced EMMF [11, 13] to the system of Equation (2). If the waveguide is excited by the H_{10} -wave with amplitude H_0 , the system of linear algebraic equations (SLAE) relative to unknown current amplitudes J_{0n} and J_{00}^s can be presented as

$$\begin{cases} J_{00}^s(Z_{00}^{sWg} + Z_{00}^{sHs}) + J_{01}Z_{01} + J_{02}Z_{02} + \dots + J_{0N}Z_{0N} = -\frac{i\omega}{2k}H_0^s, \\ J_{00}^s Z_{10} + J_{01}(Z_{11} + F_1^{\bar{Z}}) + J_{02}Z_{12} + \dots + J_{0N}Z_{1N} = 0, \\ J_{00}^s Z_{20} + J_{01}Z_{21} + J_{02}(Z_{22} + F_2^{\bar{Z}}) + \dots + J_{0N}Z_{2N} = 0, \\ \dots \\ J_{00}^s Z_{N0} + J_{01}Z_{N1} + \dots + J_{0(N-1)}Z_{N(N-1)} + J_{0N}(Z_{NN} + F_N^{\bar{Z}}) = 0, \end{cases} \quad (4)$$

where $H_0^s = H_0 \int_{-L_0}^{L_0} \cos \frac{\pi s_0}{a} f_0^s(s_0) ds_0$, Z_{mn} and $F_n^{\bar{Z}}$ are dimensionless coefficients. For example, the expression for the Z_{mn} coefficients can be written as

$$Z_{mn} = \int_{-L_m}^{L_m} f_m(s_m) \left(\frac{d^2}{ds_m^2} + k^2 \right) \int_{-L_n}^{L_n} f_n(s'_n) G_{s_n}^{HsE}(s_m, s'_n) ds'_n ds_m, \quad n = 1, 2, \dots, N; \quad m = 1, 2, \dots, N; \quad (5)$$

which can be interpreted as the vibrator own or mutual effective resistances if $n = m$ or $n \neq m$.

The electrodynamic characteristics of the vibrator-slot antenna can be found by solving SLAE in Eq. (4) relative to the currents amplitudes J_{0n} and J_{00}^s . For example, the field reflection coefficient S_{11} defined by the slot inhomogeneity in the semi-infinite rectangular waveguide operating in the single-mode regime can be presented as

$$S_{11} = \left\{ 1 - \frac{16\pi\gamma J_{00}^s}{abk\omega H_0} \cdot \frac{\sin kL_0 \cos \frac{\pi L_0}{a} - \frac{ka}{\pi} \cos kL_0 \sin \frac{\pi L_0}{a}}{1 - \left[\frac{\pi}{ka} \right]^2} \right\} e^{2i\gamma z}, \quad (6)$$

where $\gamma = \sqrt{k^2 - (\pi/a)^2}$ is the propagation constant. The power reflection coefficient $|S_{\Sigma}|^2$ of the slot into the half-space can be obtained by using the energy balance equation

$$|S_{11}|^2 + |S_{\Sigma}|^2 = 1. \quad (7)$$

Let us introduce a system of spherical coordinates shown in Fig. 1. The total wave zone field ($R \gg \lambda$) reradiated by the combined vibrator director array equal to the sum of the secondary radiation fields of each vibrator taking into account the phases of fields arriving to the observation point $C(R, \theta, \varphi)$ can be written as

$$\begin{aligned} \vec{E}(R, \theta, \varphi) = & \frac{2k^2 e^{-ikR}}{\omega R} \left[i \left(\vec{\theta}^0 \sin \varphi + \vec{\varphi}^0 \cos \theta \cos \varphi \right) J_{00}^s F_{C0} \right. \\ & \left. + \left(\vec{\theta}^0 \cos \theta \sin \varphi + \vec{\varphi}^0 \cos \varphi \right) \sum_{n=1}^N J_{0n} F_{Cn} \sin(kz_n \cos \theta) \right], \quad (8) \end{aligned}$$

where $\vec{\theta}^0$ and $\vec{\varphi}^0$ are the unit vectors, $F_{C0} = \int_{-L_0}^{L_0} f_0^s(x) e^{iks_0 \sin \theta \cos \varphi} ds_0$, and $F_{Cn} = \int_{-L_n}^{L_n} f_n(s_n) e^{ik_n \sin \theta \sin \varphi} ds_n$. If the relation in Eq. (3) is taken into account, function F_{C0} can be written

as

$$F_{C0} = \frac{2}{k^2 - (k \sin \theta \cos \varphi)^2} [k \cos(kL_0 \sin \theta \cos \varphi) \sin(kL_0) - k \sin(kL_0 \sin \theta \cos \varphi) \cos(kL_0) \sin \theta \cos \varphi] - 2L_0 \cos(kL_0) \frac{\sin(kL_0 \sin \theta \cos \varphi)}{kL_0 \sin \theta \cos \varphi}, \quad (9a)$$

$$F_{Cn} = \frac{2}{\tilde{k}_n^2 - (k \sin \theta \sin \varphi)^2} [\tilde{k}_n \cos(kL_n \sin \theta \sin \varphi) \sin(\tilde{k}_n L_n) - k \sin(kL_n \sin \theta \sin \varphi) \cos(\tilde{k}_n L_n) \sin \theta \sin \varphi] - 2L_n \cos(\tilde{k}_n L_n) \frac{\sin(kL_n \sin \theta \sin \varphi)}{kL_n \sin \theta \sin \varphi}. \quad (9b)$$

As can be seen from expressions (8) and (9), the E -plane ($\varphi = 90^\circ$) and H -plane ($\varphi = 0^\circ$) components of the electric field are $E_\varphi = 0$ and $E_\theta = 0$. The longitudinal component of the field in the far zone is $E_r = 0$.

3. NUMERICAL RESULTS

The electrodynamic characteristics were simulated for the YUCVSRS consisting of rectangular waveguide and N vibrator directors. The waveguide was excited by the H_{10} -wave with amplitude $H_0 = 1$ at the frequency $f = 9.2$ GHz ($\lambda = 32.6$ mm). The waveguide cross-section, wall thickness, slot width, and the radii of the perfectly conducting vibrators ($z_{in}^{av} = 0$) where $a \times b = 23 \times 10$ mm², $h = 1$ mm, $d = 1.5$ mm, and $r_n = 0.4$ mm. The remaining parameters of the YUCVSRS: the slot length, vibrator length, and distances between structural elements were selected by the numerical optimization to ensure the maximum directivity D in the direction of $\{0z\}$ axis under condition of satisfactory waveguide matching (the voltage standing wave ratio VSWR < 1.1). The directivity D and VSWR were calculated by the following relationships:

$$\text{VSWR} = \frac{1 + |S_{11}|}{1 - |S_{11}|}, \quad (10)$$

$$D = \frac{4\pi}{\int_0^{2\pi} \int_0^{\pi/2} [F(\theta, \varphi)]^2 \sin \theta d\theta d\varphi} \quad (11)$$

where $F(\theta, \varphi) = \frac{|\vec{E}(R, \theta, \varphi)|}{|\vec{E}(R, \theta_m, \varphi_m)|}$ is the radiation pattern (RP) normalized at the electric field modulus in the radiation maximum direction.

The YUCVSRS optimization was carried out under the condition that all its vibrator directors are positions at equal distances $\Delta z = z_1 = z_{n+1} - z_n$ from each other. The optimal parameters of the YUCVSRS: $2L_0$, $2L_n$ and Δz for different number of vibrator directors are shown in Table 1.

The calculated RPs in the main polarization planes for the optimized YUCVSRS, the angular plots $|F| = |E_\theta(\theta, \varphi = 0^\circ)|$ and $|F| = |E_\varphi(\theta, \varphi = 90^\circ)|$, are presented in Fig. 2. All plots are normalized to

Table 1. Parameters of the YUCVSRS.

N	D	$2L_0$	$2L_n$	Δz
1	6.89	0.521 λ	0.398 λ	0.269 λ
2	11.90	0.536 λ	0.405 λ	0.294 λ
3	16.13	0.54 λ	0.406 λ	0.321 λ
4	19.73	0.528 λ	0.402 λ	0.349 λ
5	22.97	0.518 λ	0.399 λ	0.367 λ

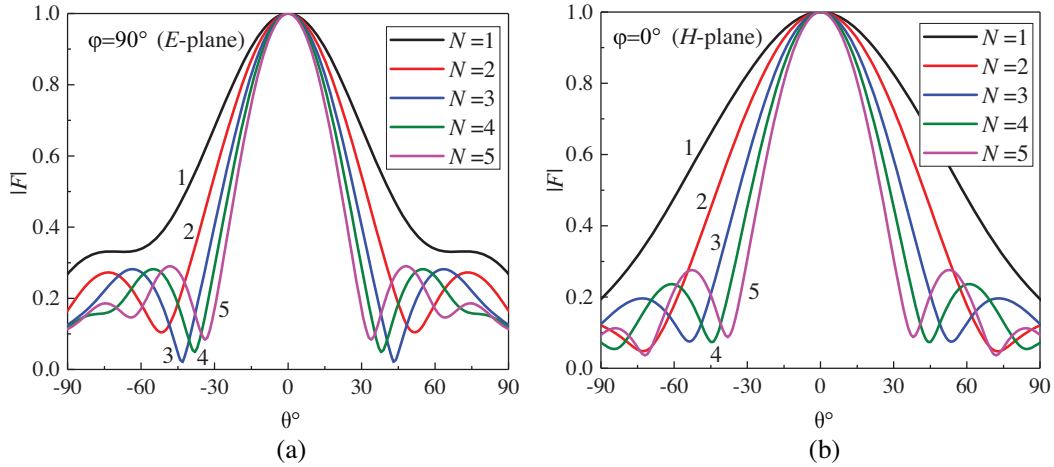


Figure 2. The RPs of the YUCVSRS with various vibrator numbers.

the maximum of the electric field modulus for a particular antenna structure. As can be seen from Fig. 2, the main lobe of the RP becomes narrower if the number of vibrator elements is increased. At the same time, the widths of the RP main lobes (at the level $|F| = 0.5$) in the orthogonal polarization planes tend to approach one another. As shown in [15], the two-element vibrator-slot system with a vibrator director, whose length was $2L_1 = 0.407\lambda$, and the distance between the resonant slot and vibrators was $\Delta z = 0.105\lambda$, is characterized by almost identical RPs in E - and H -planes. This effect was experimentally proved in [15]. The simulation results obtained for the two-element YUCVSRS have confirmed the similarity of the RP in the two polarization planes. Thus, the validity of the mathematical model and its physical adequacy are proved.

Properties of the side radiation for the optimized YUCVSRS can be analyzed by comparing the RPs for $N = 2$, $N = 3$, $N = 4$, and $N = 5$ presented in Fig. 3. As can be seen, if the number of radiating elements in the YUCVSRS is increased, the number of RP side lobes also increases in accordance with electrodynamics principles. It is also established that the power levels for the side lobes do not exceed 10% of that for the main lobe.

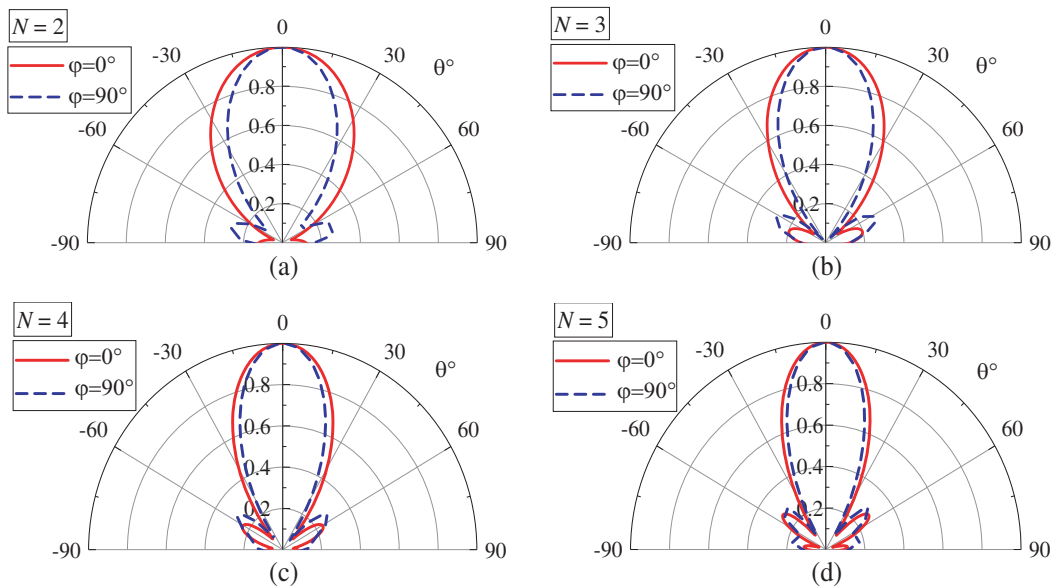


Figure 3. The RPs of the YUCVSRS with optimized parameters.

The internal and external energy characteristics of the YUCVSRS with the parameters listed in Table 1 are presented in Fig. 4. The frequency plots of the coefficients $|S_{11}|$, $|S_{\Sigma}|^2$, and VSWR defined by formulas (6), (7), and (11) for different N are shown in Fig. 4(a). The frequency plots of the directivity D [dB] (11) and the antenna gain G defined by the formula

$$G = D \cdot |S_{\Sigma}|^2 \tag{12}$$

are presented in Fig. 4(b).

The plots shown in Fig. 4 are calculated in the frequency range $f \in [7.5; 10.5]$ GHz belonging to the single-mode waveguide regime. As can be seen, the curves $|S_{11}|$, VSWR have maxima, and the curves $|S_{\Sigma}|^2$, D and G have minima in the vicinity of the frequency $f = 9.2$ GHz. It can also be stated that if

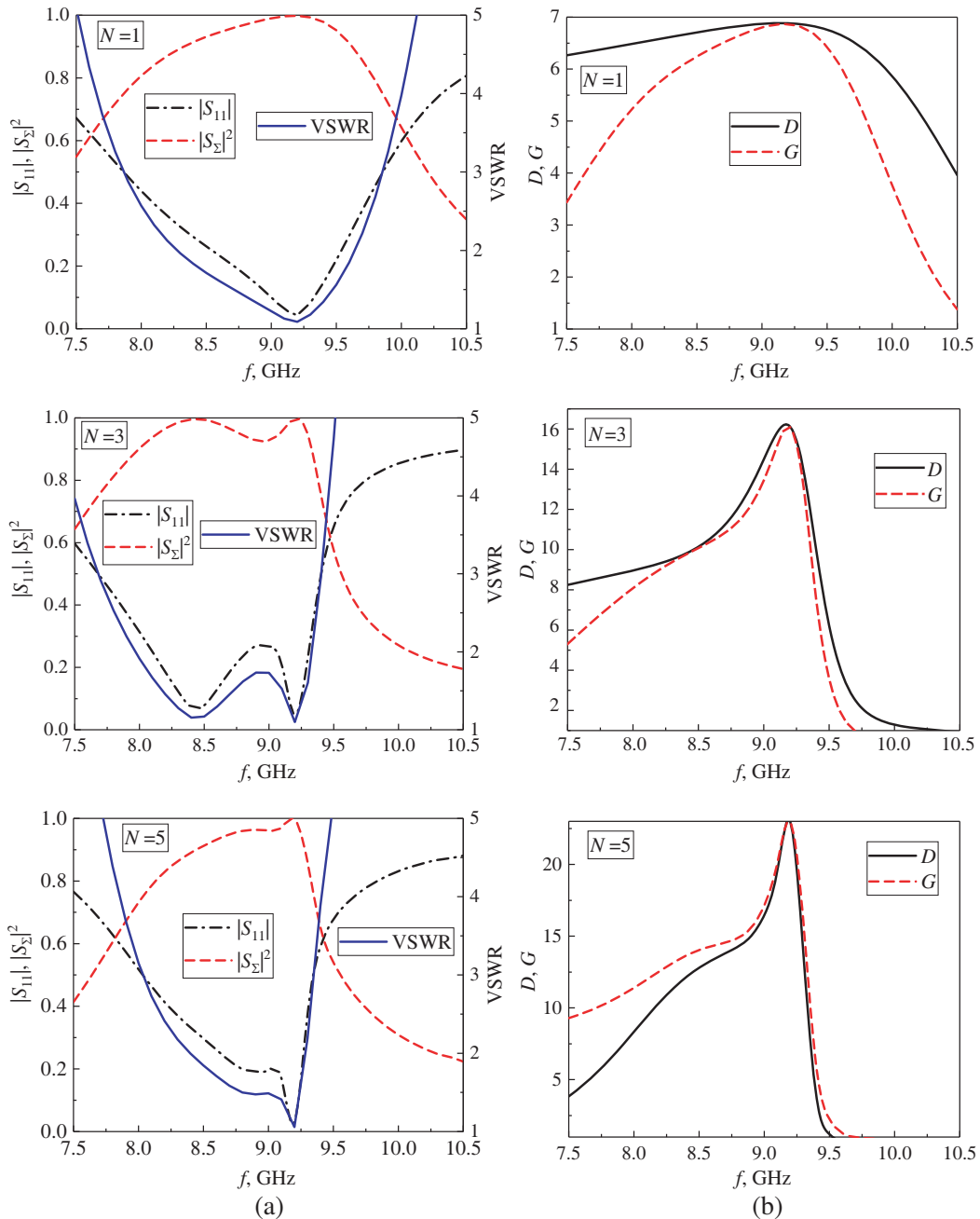


Figure 4. The frequency plots of the energy characteristics for the YUCVSRS with various N .

the number of vibrators is increased, the operating frequency band becomes narrower.

The simulation results have confirmed the possibility of reducing the main lobe width and increasing its directivity and gain by using the system of several passive vibrator directors arranged in the Yagi-Uda configuration. It is shown that the YUCVSRS with optimized parameters can provide the maximum directivity and good matching of the waveguide transmission line with $VSWR < 1.1$.

4. CONCLUSION

The problem of electromagnetic wave radiation by the YUCVSRS consisting of a rectilinear narrow slot cut in the end wall of the rectangular waveguide and several impedance vibrators placed above the infinite screen has been solved by the generalized method of induced EMMF in the self-consistent formulation. The YUCVSRS allows us to obtain narrower RP than that of a stand-alone slot. The electro-dynamically rigorous approach is based on the application of the functional current distributions obtained as the analytical solution of the integral equations for currents by the asymptotic averaging method for the stand-alone impedance vibrator and slot.

Mathematical modeling of the internal and external electrodynamic characteristics was carried out for the YUCVSRS with several perfectly conducting identical vibrator directors. It has been shown that in narrow frequency bands, the YUCVSRS with optimized parameters allow us to obtain the maximum directivity with satisfactory matching of the waveguide transmission line.

Thus, the numerical results have confirmed the possibility to develop the combined vibrator-slot radiating structure of the Yagi-Uda type, operating in the microwave and EHF wave bands. It should be emphasized that the YUCVSRS with vibrators characterized by different types of impedances can be investigated within the framework of the presented model. The use of such vibrators allows us to vary the electrical length of the vibrator directors to decrease the antenna dimensions in the centimeter wavelength range and to increase them to ensure the physical implementation of the antenna in millimeter range.

REFERENCES

1. Yagi, H. and S. Uda, "Projector of the sharpest beam of electric waves," *Proc. Imperial Academy Japan*, Vol. 2, 49–52, 1926.
2. Balanis, C. A., *Antenna Theory: Analysis and Design*, John Wiley & Sons Inc., New York, 2005.
3. King, R. W. P., R. B. Mack, and S. S. Sandler, *Arrays of Cylindrical Dipoles*, Cambridge University Press, New York, 1968.
4. Berdnik, S. L., V. A. Katrich, M. V. Nesterenko, and Y. M. Penkin, "Electromagnetic waves radiation by a vibrators system with variable surface impedance," *Progress In Electromagnetics Research M*, Vol. 51, 157–163, 2016.
5. Campbell, R. W., "Endfire antenna array having loop directors," U.S. Patent 3,491,361, issued January 20, 1970.
6. Petlya, I. I. and V. A. Panchenko, "Loop antenna," RF Patent 2174272, issued September 27, 2001.
7. Liu, H., S. Gao, and T.-H. Loh, "Small director array for low-profile smart antennas achieving higher gain," *IEEE Trans. Antennas Propag.*, Vol. 61, 162–168, 2013.
8. Wang, Z., X. L. Liu, Y.-Z. Yin, J. H. Wang, and Z. Li, "A novel design of folded dipole for broadband printed Yagi-Uda antenna," *Progress In Electromagnetics Research C*, Vol. 46, 23–30, 2014.
9. Altshuler, E. E., "A monopole array driven from a rectangular waveguide," *IRE Trans. Antennas Propag.*, Vol. 10, 558–560, 1962.
10. Zhang, Z., X.-Y. Cao, J. Gao, S.-J. Li, and X. Liu, "Compact microstrip magnetic Yagi antenna and array with vertical polarization based on substrate integrated waveguide," *Progress In Electromagnetics Research C*, Vol. 59, 135–141, 2015.

11. Berdnik, S. L., V. A. Katrich, M. V. Nesterenko, Yu. M. Penkin, and D. Yu. Penkin, "Radiation and scattering of electromagnetic waves by a multielement vibrator-slot structure in a rectangular waveguide," *IEEE Trans. Antennas Propag.*, Vol. 63, No. 9, 4256–4259, 2015.
12. Nesterenko, M. V., V. A. Katrich, Y. M. Penkin, V. M. Dakhov, and S. L. Berdnik, *Thin Impedance Vibrators. Theory and Applications*, Springer Science + Business Media, New York, 2011.
13. Penkin, D. Y., S. L. Berdnik, V. A. Katrich, M. V. Nesterenko, and V. I. Kijko, "Electromagnetic fields excitation by a multielement vibrator-slot structures in coupled electrodynamic volumes," *Progress In Electromagnetics Research B*, Vol. 49, 235–252, 2013.
14. Nesterenko, M. V., V. A. Katrich, Yu. M. Penkin, and S. L. Berdnik, *Analytical and Hybrid Methods in Theory of Slot-Hole Coupling of Electrodynamic Volumes*, Springer Science + Business Media, New York, 2008.
15. Lee, Y.-H., D.-H. Hong, and J.-W. Ra, "Waveguide slot antenna with a coupled dipole above the slot," *Electronics Lett.*, Vol. 19, No. 8, 280–282, 1983.